IEEE Access
Multidisciplinary | Rapid Review | Open Access Journal

SPECIAL SECTION ON COMPLEX SYSTEM HEALTH MANAGEMENT BASED ON CONDITION MONITORING AND TEST DATA

Received July 20, 2017, accepted August 17, 2017, date of publication August 22, 2017, date of current version September 19, 2017.

*Digital Object Identifier 10.1109/ACCESS.2017.2743115*

# Theoretical and Experimental Studies of Localization Methodology for AE and Microseismic Sources Without Pre-Measured Wave Velocity in Mines

**LONGJUN DONG, (Member, IEEE), DAOYUAN SUN, XIBING LI, AND KUN DU**
School of Resources and Safety Engineering, Central South University, Changsha 410083, China

Corresponding author: Longjun Dong (lj.dong@csu.edu.cn)

This work was supported in part by the National Natural Science Foundation of China under Grant 41630642 and Grant 51504288, in part by the National Basic Research Program of China under Grant 2015CB060200, in part by the China Postdoctoral Science Foundation under Grant 2015M570688 and Grant 2016T90639, in part by the Young Elite Scientists Sponsorship Program by CAST under Grant 2016QNRC001, and in part by the Innovation-Driven Project of Central South University under Grant 2016CXS001.

**ABSTRACT** The acoustic emission (AE) and microseismic (MS) monitoring are efficient methods to detect faults/breaking signals for both healthy evaluation and disaster control in mining engineering. This paper presents an MS or AE source location method without the need for a pre-measured wave velocity. It can eliminate the location errors for MS/AE monitoring systems caused by the deviations of the wave velocity. To verify the applicability of the proposed method, first, tests of both the pencil lead break and the thermal fracture in granite were carried out, and location errors were compared and analyzed. Results show that the location accuracy of the proposed method is significantly improved, which is superior to the results of the traditional location method (TM) using pre-measured wave velocity. Second, blasting experiments were carried out in Dongguashan copper mine in China. The blasts were used as simulated seismic sources. Average values of absolute distance errors of the MS/AE source locations resulting from the proposed method without wave velocity and the traditional method using average measured wave velocity are 10.16 and 17.55 m, respectively. It shows that the calculated locations by the proposed method are in better agreement with the real blast coordinates. Third, the proposed method is also applied to previously published data. It gives superior results compared with the considered existing methods. Results of the pencil lead break tests, the thermal fracture experiment in granite, and the blasting experiments (including published data) have demonstrated that the proposed method can not only decrease the location errors induced by measurement deviation of velocity, but also locate the MS/AE source in real time, which is a beneficial complement to the method TM in mines.

**INDEX TERMS** Localization method, microseismic/AE sources, fault detection, wave velocity.

## I. INTRODUCTION

Many countries, such as South Africa, Poland, Russia, Canada, the United States, Australia, China, India, Chile, Germany and Japan, etc., have experienced different rockburst hazards at different times in some mines and tunnels [1]–[9].

Geophysical methods, such as microseismic monitoring, geotomography, and in-seam seismic techniques, have shown an increasing significance in rock physical mechanics and mining engineering in recent decades [6], [8], [10]–[13]. In particular, the microseismic or acoustic emission(MS/AE) monitoring is widely used to locate faults/breaking signals in tunneling and mining engineering, which provide a scientific basis for evaluating the rockbursts and seismic hazards [14]–[17].

It is crucial that the localization methodology has a reasonable location accuracy, which can provide key information for controlling rockbursts and improving the safety performance in deep mining engineering. Many researchers have developed MS/AE source location

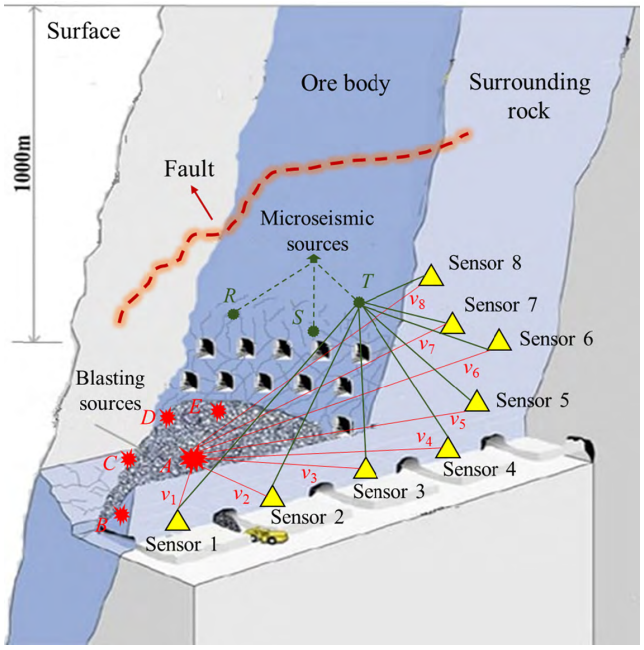


**FIGURE 1.** Upper graph shows an example for the propagation paths of *P*-wave with blasting sources and microseismic sources located at different coordinates. In the traditional methods such as STT and STD methods, the average velocity of blasting source *A* is equal to the average value of $v_1$ to $v_8$, which is calculated through their own distances and travel times. However, the average velocity values of other blasting source *B*, *C*, *D*, and *E* will not equal to the source *A* due to the anisotropy of rock. Similarly, the authentic velocity value of a microseismic source is not equal to the velocity value used in the localization process. Thus, it is inaccurate that locating sources using the pre-measured average velocity value of the blasting sources, where the velocity paths are different from the sources to be located.

techniques [10], [11], [18]–[27], some of which are mature technologies and are widely used in the positioning of MS/AE source. However, for most of the technologies based on the MS/AE source, a given wave velocity or practical pre-measured wave velocity of the propagation medium is required. It is well known that the wave velocity is influenced by the materials, size and surface conditions of transmission media and other factors [28], [29]. When the input wave velocity is different from the real wave velocity of the measured object, an error would occur in the system [30]. Firstly, the average wave velocity is different from that of the various regions, and the actual location of the occurrence of rockburst is not necessary in the pre-determined wave velocity area in mines (Fig.1 [29]). Secondly, the measured wave velocity is significantly affected by the distance between sensors; the measured P–wave velocity of the general container is between 2800 and 3100 m $s^{-1}$ when the distance is large; while that is about 5000 to 6000 m·$s^{-1}$ when the distance is small [31]. For instance, in Dongguashan blasting tests, the measured minimum wave velocity is 4.4 m/ms, while the maximum is 5.9 m/ms, and the average floating error of velocity is from 3% to 7% [7]. Moreover, floating rates of velocity in different regions would be much larger. In these situations, the location accuracy of the traditional location method (TM) using pre-measured wave velocity is seriously limited by the severe challenge of finding an accurate wave velocity.

A large location error can be induced by the inaccurate average wave velocity. Since these conditions result in some errors between the pre-measured wave velocity as an input of the positioning system and the actual wave velocity of the area where the rockburst occurs, it would result in a large location error [31]. Generally, the location errors caused by measurement deviations of the wave velocity are from 10 to 100m [32], which would seriously affect the accuracy of rockburst early warning.

To eliminate the location errors for microseismic monitoring systems due to temporal and spatial errors of the microseismic wave velocity, Dong *et al.* [23] discussed three different possible mathematical functions for the microseismic source location in the unknown wave velocity conditions. In this paper, a microseismic source location method without the pre-measured wave velocity (MSLM-WV) was presented. The pencil lead break tests, the thermal fracture in granite, and the blast experiments were used to verify the proposed MSLM-WV method.

## II. METHODOLOGIES

### A. REVIEWS OF TRADITIONAL METHOD (TM)

An iterative, linearized least-squares location method was introduced as early as 1910 by Ludwig Geiger, and is still widely used in earthquake and microseismic sources location [22]. In a MS/AE source location method, the sensors are placed in a location area, and are not in the same plane. Three-dimensional coordinates of the sensors are known, which are expressed as $(x_1, y_1, z_1)$, $(x_2, y_2, z_2)$, ..., $(x_N, y_N, z_N)$, and $N$ is the number of sensors. When a MS/AE event occurs, the sensors receive the source signals and record the arrival times, such as $t_1, t_2, \ldots, t_N$. Suppose that the arrival time of the $k$-th sensor is

$$t_k = t_0 + \frac{\sqrt{(x_k - x_0)^2 + (y_k - y_0)^2 + (z_k - z_0)^2}}{c_{\text{con}}} \tag{1}$$

where $t_0$ is the origin time of the MS/AE event; $(x_k, y_k, z_k)$ are the coordinates of the $k$-th sensor; $(x_0, y_0, z_0)$ are the coordinates of microseismic source location; and $c_{\text{con}}$ is the pre-determined average equivalent wave velocity of P wave propagation in the medium.

The difference of observed arrival times between two different sensors $i$ and $j$ is expressed as

$$\Delta t_{ij} = t_i - t_j = \frac{l_i - l_j}{c_{\text{con}}} \tag{2}$$

$$l_i = \sqrt{(x_i - x_0)^2 + (y_i - y_0)^2 + (z_i - z_0)^2} \tag{2a}$$

$$l_j = \sqrt{(x_j - x_0)^2 + (y_j - y_0)^2 + (z_j - z_0)^2} \tag{2b}$$

where $(x_i, y_i, z_i)$ and $(x_j, y_j, z_j)$ are the coordinates of the $i$-th and $j$-th sensors, respectively; $t_i$ and $t_j$ are the arrival times of the $i$-th and $j$-th sensors, respectively.

In the traditional method (TM), Equation (2a) is rewritten as

$$\Delta t_{ij} = f(x_i, y_i, z_i, x_j, y_j, z_j, x_0, y_0, z_0, c_{con}) \tag{3}$$

In Equation (3), $(x_i, y_i, z_i)$, $(x_j, y_j, z_j)$, as well as $c_{\text{con}}$ are independent variables, and $\Delta t_{ij}$ is a dependent variable, which are known parameters, whereas $(x_0, y_0, z_0)$ are unknown parameters in the TM. There are three unknown parameters in the problem. Therefore, more than three sensors are needed to obtain the solutions by solving the nonlinear equations.

### B. AN INNOVATIVE MICROSEISMIC SOURCE LOCATION METHOD WITHOUT PRE-MEASURED WAVE VELOCITY

To improve the location accuracy, the known parameters of equations should not include the pre-determined wave velocity. Therefore, the difference of observed arrival times between two different sensors $i$ and $j$ is expressed as

$$\Delta t_{ij} = t_i - t_j = \frac{l_i - l_j}{c} \tag{4}$$

where the average equivalent wave velocity $c$ is an unknown parameter, which is different from $c_{\text{con}}$ in Equations (2a) and (3).

Equation (4) can be rewritten as

$$\Delta t_{ij} = f(x_i, y_i, z_i, x_j, y_j, z_j, x_0, y_0, z_0, c) \tag{5}$$

In Equation (5), the independent variables $(x_i, y_i, z_i)$, $(x_j, y_j, z_j)$, and the dependent variable $\Delta t_{ij}$ are known parameters, and $x_0, y_0, z_0, c$ are unknown parameters. Since there are four unknown parameters, more than four sensors are needed to obtain the solutions by solving the nonlinear equations. The clear difference from the TM is that it does not need a pre-measured wave velocity. This method is called MSLM-WV (Microseismic Source Location Method Without the Pre-measured Wave Velocity).

The solving methods of the TM and MSLM-WV are similar, which are nonlinear fitting problems with a single dependent variable.According to all the observed data $(x_i, y_i, z_i; x_j, y_j, z_j)$, the Equation (5) can determine a regression value

$$\Delta \hat{t}_{ij} = f(x_i, y_i, z_i, x_j, y_j, z_j, x_0, y_0, z_0, c) \tag{6}$$

The difference between $\Delta \hat{t}_{ij}$ and $\Delta t_{ij}$ can describe the degree of deviation between the regression value and observed values.

Due to $(x_i, y_i, z_i; x_j, y_j, z_j)$, if the degree of deviation between $\Delta t_{ij}$ and $\Delta \hat{t}_{ij}$ is smaller, it shows that the fitted line and experimental points could fit better. The sum of squared deviations of all observations and fitted values is

$$Q(x_0, y_0, z_0, c) = \sum_{i,j=1}^{n} \left[\Delta \hat{t}_{ij} - \Delta t_{ij}\right]^2 \tag{7}$$

Equation (7) describes the deviations between all observed and experimental values. Therefore, the source parameters $(x_0, y_0, z_0, c)$ can be solved out if the $Q(x_0, y_0, z_0, c)$ reaches a minimum:

$$Q(x_0, y_0, z_0, c) = \sum_{i,j=1}^{n} \left[\Delta \hat{t}_{ij} - \Delta t_{ij}\right]^2 = \min \tag{8}$$

Since Equation (8) is the second non-negative function of $x_0$, $y_0$, $z_0$, $c$, it always has the minimum. The coordinates of the MS/AE source location and the P wave velocity (i.e. $x_0, y_0, z_0, c$) can be obtained by solving Equation (8). For a simple source location problem, only $x_0$, $y_0$, $z_0$ should be solved. Equation (8) is a nonlinear fitting problem with a single dependent variable.

The common nonlinear fitting methods include the Levenberg-Marquardt method (LM), the Nelder Mead's simplex method, the gradient descent method, as well as the Gauss-Newton method. Nelder Mead's simplex method is a direct search method [33]. Its computational process is simple and it does not require calculation of derivatives [34]. However, Nelder Mead's simplex method does not rely on the gradient so it may converge slowly or may not converge at all. This scenario is not uncommon and remarkably reduces the efficiency of Nelder Mead's simplex method in solving complicated problems such as optimizing multi-dimensional source locations or training neural networks.

In the gradient descent method, the sum of the squared errors is reduced by updating the parameters in the direction of the greatest reduction of the least squares objective.

In the Gauss-Newton method, the sum of the squared errors is reduced by assuming that the least squares function is locally quadratic, and finding the minimum of the quadratic.

The LM algorithm is an iterative technique that locates the minimum of a multivariate function that is expressed as the sum of squares of non-linear real-valued functions [35], [36]. It has become a standard technique for non-linear least-squares problems, widely adopted in a broad spectrum of disciplines. The LM method acts more like a gradient-descent method when the parameters are far from their optimal value, and acts more like the Gauss-Newton method when the parameters are close to their optimal value. Therefore, in this paper, the LM method was applied to solve the optimum MS/AE source locations.

## III. AE EXPERIMENTS IN ROCKS

A cuboid size granite sample was used to conduct the experiments, with the dimension of 63 × 43 × 10 cm. Before starting the experiment, the upper surface was meshed into 35 grids and the grid lines were extended to the side faces $F_1$ to $F_4$. Other four lines were marked out 4 cm under the upper surface forming 48 grids, of which six points were used to arrange the AE sensors. Another six randomly selected points of the grids, 3, 9, 10, 14, 15 and 17, were used to carry out pencil lead break tests. The end vertex in lower left corner of the upper surface was set as the origin of the coordinate, the actual arrangements are shown in Fig. 2.

After connecting and opening all the devices, a fire of liquefied gas was lit to heat the lower surface of the sample.

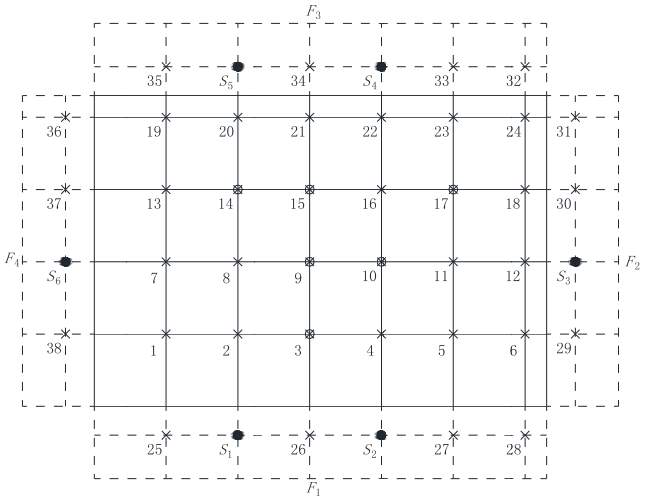


**FIGURE 2.** Location of the AE sensors and pencil lead break points (the solid line shows the layout of the upper surface and the dotted line shows the layout of the side faces $F_1$ to $F_4$, $S_1$ to $S_6$ are the location of the AE sensors, points 3, 9, 10, 14, 15 and 17 are the location of pencil lead break tests).

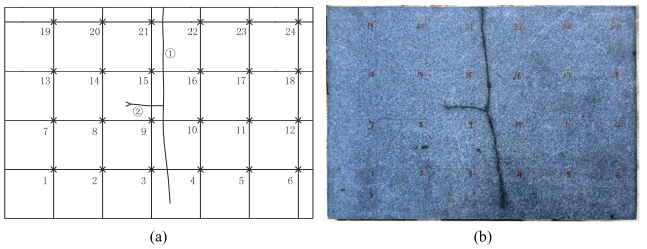


**FIGURE 3.** Actual occurrence and extension of cracks (① indicates the first crack and ② indicates the second one): (a) shows the fault location in grids, and (b) shows practical faults in the granite sample.

Five minutes later, a crack about 20cm from $F1$ to the center of the sample occurs with a loud noise. With the heating process continues, the temperature of the sample increases gradually, but the crack extends rapidly. Another ten minutes later, the second crack occurs. After heating about fifty minutes, the second crack forks into two directions. In the next two hours, the cracks extend slowly. The heating progress was terminated until the extending cracks were invisible. The actual occurrence and the extended faults are shown in Fig. 3.

In the experiment, pencil lead break tests were used to validate the proposed MSLM-WV method and analyze location errors. The six pencil lead break tests source location were calculated by the MSLM-WV method using the arrivals and coordinates of sensors, and the located results and errors are listed in Table 1.

From the Table 1, it shows that the calculated coordinates using the MSLM-WV method are more consistent with practical coordinates. The minimum and maximum absolute errors of $X$ coordinates are 0.56 and 4.82cm, the minimum and maximum absolute errors of $Y$ coordinates are 0.66 and 4.69 cm, respectively. The average errors of $X$ and $Y$ using MSLM-WV are 2.29 and 2.95cm, respectively, which are smaller than the errors of 7.04 and 4.82cm using the TM.

The located results for fault location of the thermal fracture experiment are shown in Fig. 4. The points indicate AE events of thermal fracture. Fig. 4 clearly indicates that most AE events of the thermal fracture occur in the center of the granite sample. It has the tendency to extend to the direction of $F1$ and $F4$, and the tendency is consistent with the actual situation shown in Fig. 2. From Fig. 4, graphs (a) and (b) show the coordinates $X$ and $Y$ with the colorbar, which indicates the amplitude of the events using the TM and MSLM-WV, respectively; Graphs (c) and (d) show the coordinates $X$ and $Y$ with the colorbar, which indicates coordinates $Z$ using the TM and MSLM-WV, respectively; and graphs (e) and (f) show the coordinates $X$ and $Y$ with the colorbar, which indicates the amplitude of events using the TM and MSLM-WV, respectively. They show that the located events of the MSLM-WV are more accurate than the results of the TM, which is much closer to the practical faults in the granite sample shown in Fig. 3(b).

The visible and simple fact is the fire of liquefied gas heat the lower surface of the granite sample (the plane with $Z = 0$), which can induce numerous AE events in the lower surface. It is consistent with the results of the graph (f) using the MSLM-WV, while the AE events of graph (e) are very scare in the lower surface. Both pencil lead break tests and the thermal fracture experiment have proved that the proposed method without the need for a premeasured wave velocity can improve the location accuracy significantly, which is superior to results of the TM using premeasured wave velocity.

## IV. VERIFICATION OF BLASTING EXPERIMENTS

### A. BLASTING EXPERIMENTS AND RESULTS

To validate the proposed MSLM-WV, blasting tests were carried out at Dongguashan copper mine. No permits were required to access the mine. The field studies did not involve endangered or protected species. The copper deposit is about 1000 m beneath the surface and it is controlled by an anticline. Its strike is NE35° −40° and the dip along the strike is about 10°. The maximum in-situ stress is 30−35 MPa, approximately parallel to the strike direction of the orebody, and the minimum in-situ stress is 9−16 MPa, approximately vertical. The ore and its surrounding rocks are very hard and prone to rockburst during mining operation [7].

The Dongguashan rockburst monitoring system has been operating since Aug. 25, 2005. It is composed of a seismic monitoring system and a conventional stress and deformation monitoring system. The seismic monitoring system was provided by ISS system from Integrated Seismic Systems International (South Africa). It has 24 channels and 16 sensors. All signals are transmitted by copper twisted cables to the monitoring control of underground, and then transmitted by an optical cable to the monitoring center on the ground

**TABLE 1.** Real coordinates and located results using methods MSLM-WV and TM.

| Event No. | Real coordinates /cm | | MSLM-WV/cm | | | | TM/cm | | | |
|---|---|---|---|---|---|---|---|---|---|---|
| | $X$ | $Y$ | $X$ | $Y$ | $E_X$ | $E_Y$ | $X$ | $Y$ | $E_X$ | $E_Y$ |
| 1 | 30 | 10 | 32.04 | 14.69 | 2.04 | 4.69 | 30.35 | 6.34 | 0.35 | 3.66 |
| 2 | 30 | 20 | 30.85 | 20.66 | 0.85 | 0.66 | 37.60 | 21.78 | 7.60 | 1.78 |
| 3 | 40 | 20 | 41.79 | 23.64 | 1.79 | 3.64 | 46.49 | 15.45 | 6.49 | 4.55 |
| 4 | 20 | 30 | 20.56 | 27.09 | 0.56 | 2.91 | 28.50 | 32.98 | 8.50 | 2.98 |
| 5 | 30 | 30 | 34.82 | 26.34 | 4.82 | 3.66 | 34.68 | 27.63 | 4.68 | 2.37 |
| 6 | 50 | 30 | 53.69 | 32.14 | 3.69 | 2.14 | 35.37 | 34.21 | 14.63 | 4.21 |
| Average | | | | | 2.29 | 2.95 | | | 7.04 | 3.26 |

**TABLE 2.** The times, locations, and amount of dynamite of blasting experiments.

| Event No. | Times | The blasting test locations | Site coordinates /m | | | Amount of dynamite /kg |
|---|---|---|---|---|---|---|
| | | | $X$ | $Y$ | $Z$ | |
| 1 | 30 August, 10:57 | −760 level 56−4 stope tunnel | 22556.2 | 84528.4 | -753.2 | 2.25 |
| 2 | 8 September,10:41 | −820 level 56−6 stope tunnel | 22570.0 | 84479.0 | -814.4 | 2.4 |
| 3 | 8 September,13:03 | −790 level 56−14 stope tunnel | 22673.0 | 84359.0 | -795.5 | 2.4 |

**TABLE 3.** Real coordinates and location results of methods MSLM-WV and TM.

| Blasting event No. | Real coordinates /m | | | MSLM-WV /m | | | TM /m | | |
|---|---|---|---|---|---|---|---|---|---|
| | $X$ | $Y$ | $Z$ | $X$ | $Y$ | $Z$ | $X$ | $Y$ | $Z$ |
| 1 | 84528.4 | 22556.2 | -753.2 | 84524.8881 | 22548.5462 | -746.2285 | 84519.8508 | 22547.4364 | -749.0477 |
| 2 | 84479.0 | 22570.0 | -814.4 | 84477.8613 | 22566.9001 | -806.6764 | 84488.3244 | 22570.7159 | -802.8833 |
| 3 | 84359.0 | 22673.0 | -795.5 | 84350.9794 | 22667.3735 | -800.7970 | 84351.9548 | 22676.1976 | -771.8323 |

**TABLE 4.** The comparisons of location errors using MSLM-WV and TM.

| Event No. | MSLM-WV /m | | | | TM /m | | | |
|---|---|---|---|---|---|---|---|---|
| | $X_{erro}$ | $Y_{erro}$ | $Z_{erro}$ | $D_{erro}$ | $X_{erro}$ | $Y_{erro}$ | $Z_{erro}$ | $D_{erro}$ |
| 1 | 3.5119 | 7.6538 | 6.9715 | 10.93233 | 8.5492 | 8.7636 | 4.1523 | 12.9279 |
| 2 | 1.1387 | 3.0999 | 7.7236 | 8.400001 | 9.3244 | 0.7159 | 11.5167 | 14.8355 |
| 3 | 8.0206 | 5.6265 | 5.297 | 11.13758 | 7.0452 | 3.1976 | 23.6677 | 24.9002 |
| Average | 4.2237 | 5.4601 | 6.6640 | 10.1566 | 8.3063 | 4.2257 | 13.1122 | 17.5545 |

surface as well as the safety and production management offices of the mine. Currently, the area of monitoring is the first mining area where there are four panels located between exploration lines 52 and 60 in the surrounding rock mass. The monitoring area will be extended to the entire mine later.

To verify the location accuracy and practicality of the MSLM-WV, blasting tests were carried out and the blasts were used to simulate the microseismic sources. The blasting test locations, times, site coordinates, and amount of ANFO are listed in Table 2. According to records of trigger times and the sensor location coordinates, the source locations of the blasts were calculated by the proposed method MSLM-WV. To compare with TM, the calculated results of MSLM-WV and TM are listed in Table 3, and the actual coordinates are also listed in Table 3. The P-wave velocity is 5732m in calculation using the TM, which is the average value of three blasting tests. The comparisons of location errors using MSLM-WV and TM are shown in Table 4.

Table 4 shows that the three direction coordinate errors and absolute distance errors from MSLM-WV are less than

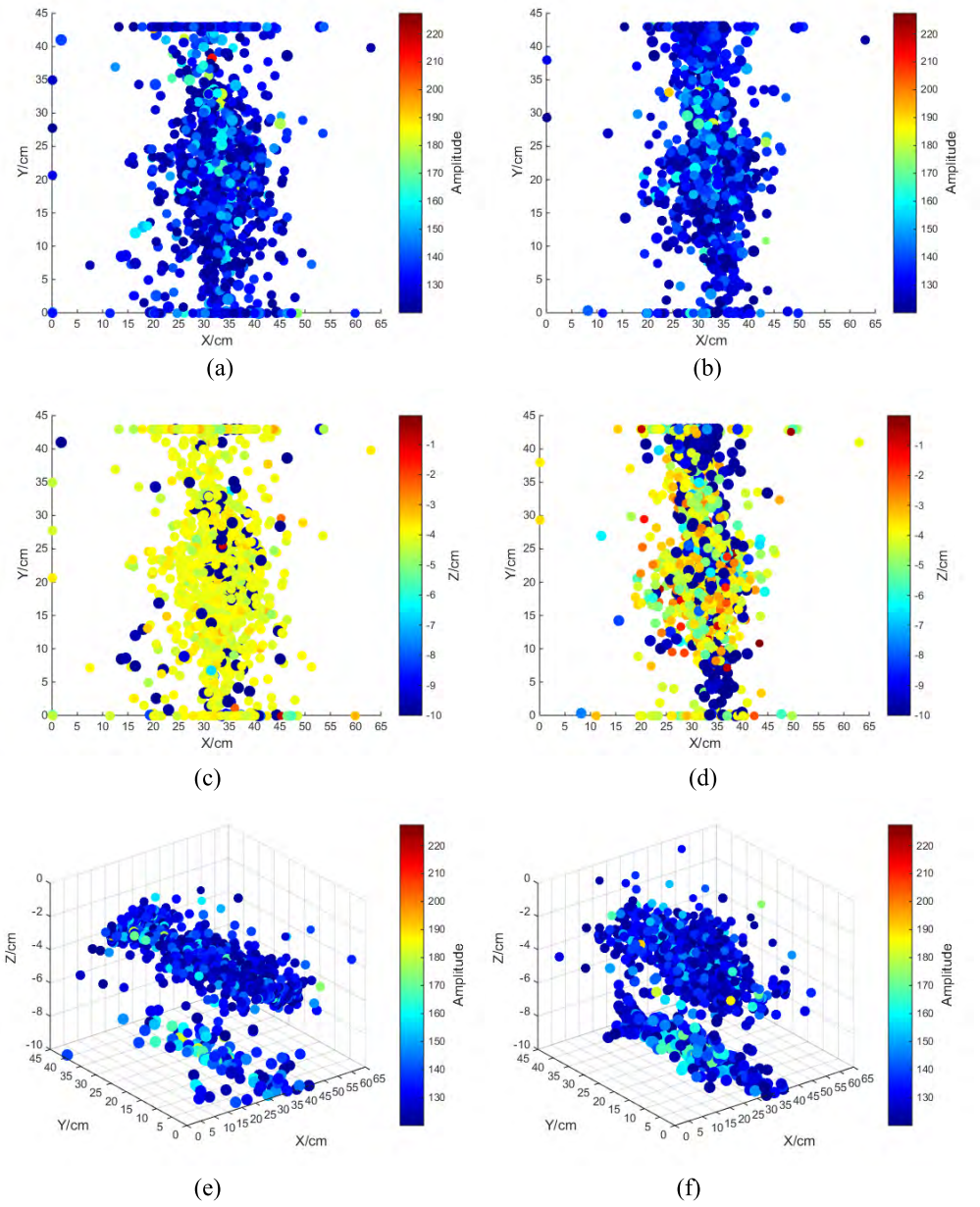


**FIGURE 4.** Upper graph shows the located results for fault location of the thermal fracture experiment, where graphs (a) and (b) show the coordinates *X* and *Y* with the colorbar indicating the amplitude of events using the methods TM and MSLM-WV, respectively; graphs (c) and (d) show the coordinates *X* and *Y* with the colorbar indicating coordinates *Z* using the methods TM and MSLM-WV, respectively; and graphs (e) and (f) show the coordinates *X*, *Y*, and *Y* with the colorbar indicating the amplitude of events using the TM and MSLM-WV, respectively.

that from the TM, and the average errors for the three axes are about 5m, and maximum is 11.14m; while the average errors of the three axes by the TM are about 8m, the maximum is 24.90m. The average error of absolute distances of MSLM-WV is 10.16m, whereas the error by the TM is 17.55m. It is concluded that the MSLM-WV is superior to the TM, and the prediction accuracy is higher than that of the TM, even when the pre-measured velocity is used in the TM.

Furthermore, to compare the fitting processes between observations and fitting values, the fitting curves from 3 blast events are shown in Fig. 5. Fig 5 with lines can be used to indicate the fitted differences of the two methods. Fig.6 gives measured value, fitted values of MSLM-WV and TM for blasting events No.1, No.2, and No.3. It can be seen that the properties of approximation for MSLM-WV is better than that of the TM. The reasons may be that the MSLM-WV can more accurately fit the relationships between the

**TABLE 5.** Sensor coordinates and arrival times for events.

| Sensor | Event 39 | | | | Sensor | Event 40 | | | |
|---|---|---|---|---|---|---|---|---|---|
| | *x* (m) | *y* (m) | *z* (m) | *t* (10 μs) | | *x* (m) | *y* (m) | *z* (m) | *t* (10 μs) |
| 52 | 5709 | 5572 | 2102 | **6820** | 52 | 5709 | 5572 | 2102 | **6055** |
| 57 | 5692 | 5559 | 2038 | 7325 | 57 | 5 692 | 5559 | 2038 | 6130 |
| 49 | 5714 | 5555 | 2140 | 7555 | 47 | 5 604 | 5635 | 2142 | 6308 |
| 59 | 5684 | 5654 | 1964 | 7620 | 59 | 5 684 | 5654 | 1964 | 6445 |
| 47 | 5604 | 5635 | 2142 | 7940 | 50 | 5 584 | 5629 | 2102 | 6790 |
| 50 | 5584 | 5629 | 2102 | 7960 | 53 | 5 639 | 5533 | 2099 | 6885 |
| 45 | 5706 | 5559 | 2197 | 8125 | 60 | 5 724 | 5555 | 1964 | 6920 |
| 53 | 5639 | 5533 | 2099 | 8130 | 45 | 5 706 | 5559 | 2197 | 7245 |
| 60 | 5724 | 5555 | 1964 | 8380 | 44 | 5 596 | 5607 | 2197 | 7390 |
| 43 | 5639 | 5555 | 2196 | 8715 | 40 | 5 628 | 5559 | 2276 | 8030 |
| 44 | 5596 | 5607 | 2197 | 8810 | 41 | 5 662 | 5581 | 2271 | 8185 |
| Sensor | Event 41 | | | | Sensor | Event 43 | | | |
| | x (m) | y (m) | z (m) | t (10 μs) | | x (m) | y (m) | z (m) | t (10 μs) |
| 57 | 5692 | 5559 | 2038 | 0 | 49 | 5714 | 5555 | 2140 | 0 |
| 59 | 5684 | 5654 | 1964 | 185 | 59 | 5684 | 5654 | 1964 | 15 |
| 47 | 5604 | 5635 | 2142 | 245 | 57 | 5692 | 5559 | 2038 | 170 |
| 50 | 5584 | 5629 | 2102 | 495 | 47 | 5604 | 5635 | 2142 | 400 |
| 53 | 5639 | 5533 | 2099 | 590 | 50 | 5584 | 5629 | 2102 | 430 |
| 60 | 5724 | 5555 | 1964 | 1070 | 53 | 5639 | 5533 | 2099 | 560 |
| 43 | 5639 | 5555 | 2196 | 1210 | 45 | 5706 | 5559 | 2197 | 565 |
| 44 | 5596 | 5607 | 2197 | 1245 | 60 | 5724 | 5555 | 1964 | 725 |
| 41 | 5662 | 5581 | 2271 | 1570 | 43 | 5639 | 5555 | 2196 | 1020 |
| 40 | 5628 | 5559 | 2276 | 1970 | 44 | 5596 | 5607 | 2197 | 1195 |
| 39 | 5608 | 5615 | 2272 | 2165 | 41 | 5662 | 5581 | 2271 | 1655 |
| | | | | | 40 | 5628 | 5559 | 2276 | 2110 |

**TABLE 6.** Source location results of MSLM-WV, TM, and methods in [37] and [38].

| Event | MSLM-WV/m | | | TM /m | | | Refs[26, 27] /m | | |
|---|---|---|---|---|---|---|---|---|---|
| | *X* | *Y* | *Z* | *X* | *Y* | *Z* | *X* | *Y* | *Z* |
| 39 | 5720.57 | 5654.34 | 2081.97 | 5720.26 | 5651.33 | 2080.57 | 5720.00 | 5651.00 | 2080.00 |
| 40 | 5715.66 | 5669.53 | 2084.39 | 5705.72 | 5671.26 | 2079.77 | 5717.00 | 5669.00 | 2084.00 |
| 41 | 5723.83 | 5661.64 | 2090.09 | 5727.39 | 5665.11 | 2092.29 | 5727.00 | 5663.00 | 2092.00 |
| 43 | 5731.60 | 5668.56 | 2083.70 | 5736.88 | 5675.25 | 2088.78 | 5736.00 | 5675.00 | 2088.00 |

**TABLE 7.** Comparisons of location errors using different methods.

| Event | MSLM-WV /m | | | | TM /m | | | | Method in Refs[37, 38] /m | | | |
|---|---|---|---|---|---|---|---|---|---|---|---|---|
| | $X_{erro}$ | $Y_{erro}$ | $Z_{erro}$ | $D_{erro}$ | $X_{erro}$ | $Y_{erro}$ | $Z_{erro}$ | $D_{erro}$ | $X_{erro}$ | $Y_{erro}$ | $Z_{erro}$ | $D_{erro}$ |
| 39 | 4.43 | 5.66 | 6.03 | **9.38** | 4.74 | 8.67 | 7.43 | **12.37** | 5.00 | 9.00 | 8.00 | **13.04** |
| 40 | 9.34 | 9.53 | 3.61 | **13.83** | 19.28 | 11.26 | 8.23 | **23.80** | 8.00 | 9.00 | 4.00 | **12.69** |
| 41 | 1.17 | 1.64 | 2.09 | **2.90** | 2.39 | 5.11 | 4.29 | **7.09** | 2.00 | 3.00 | 4.00 | **5.39** |
| 43 | 6.60 | 8.56 | 4.30 | **11.63** | 11.88 | 15.25 | 0.78 | **19.35** | 11.00 | 15.00 | 0.00 | **18.60** |

sensor coordinates and the difference of arrival times through the nonlinear algorithm. Although the basic theory of the MSLM-WV is also based on average wave velocity, it can dynamically adjust in real time, and it searches for the real time best value to meet the nonlinear relationship between the sensor coordinates and the difference of arrival times. In the

**TABLE 8.** The characteristics and comparisons of the MSLM-WV and TM methods.

| Method | Known parameters | Unknown parameters | Advantages | Disadvantages |
|---|---|---|---|---|
| TM | Coordinates of sensors; Arrivals of P-wave; Premeasured velocity | Source coordinates; Origin time of source | The minimum number of sensors is 4; | Induce locating error by the premeasured velocity; consume massive manpower and material for blasting test |
| MSLM-WV | Coordinates of sensors; Arrivals of P-wave | Source coordinates; Origin time of source; Average velocity | Weakening the locating error caused by premeasured velocity; Save manpower and material for blasting test | The minimum number of sensors is 5 |

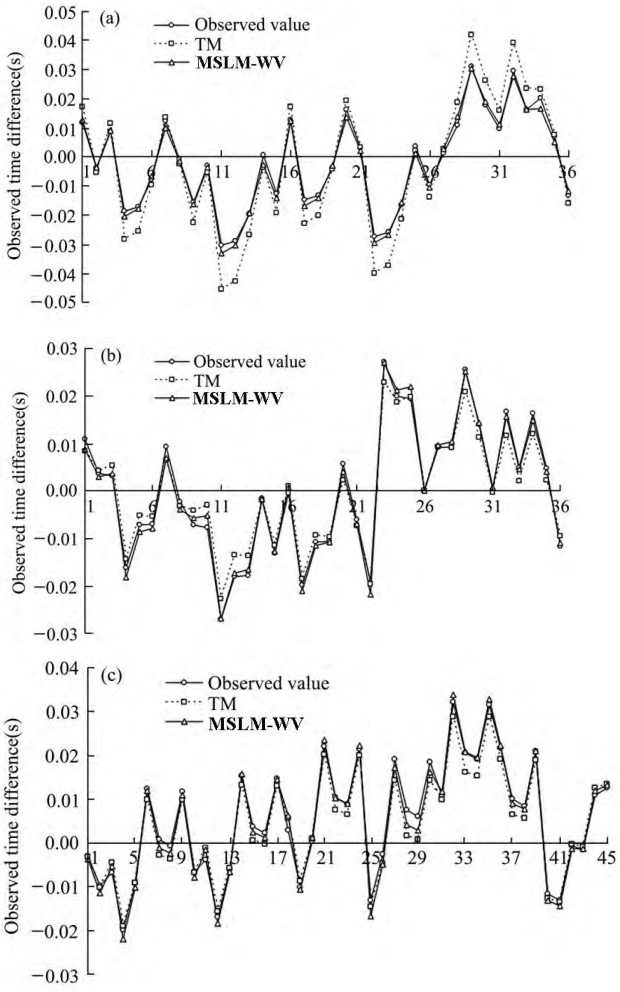


**FIGURE 5.** (a), (b), and (c) show approximations of fitting curves for blasting events No.1, No.2, No.3, respectively (note: The horizontal coordinates are the serial number for differences between arrival times).

calculating process of TM, the constant value of the wave velocity may induce large errors between the measured wave velocity in field and the real value, which would strongly affect the fitting accuracy.

### B. PUBLISHED EXAMPLE AND COMPARISONS

The published data in [37] and [38] were also used to verify the proposed method MSLM-WV. The results were compared with the results of TM and reported results in [37] and [38]. The sensor coordinates and arrival times for four events are listed in Table 5. The four major microseismic events, which caused by a nearby blast (5725m, 5660m, 2088m), were recorded during a 6 second period at a mine site. Source location results using the proposed method MSLM-WV, TM and the methods in [37] and [38] are shown in Table 6. Location errors of $X$, $Y$, $Z$ as well as absolute distance error are listed in Table 7.

In Table 7, the source location results in [37] and [38] were obtained on the condition that the blast site (5725m, 5660m, 2088m) was used as an approximation of the origin of these events. However, in practical applications, the real microseismic source location is unknown. Source location results are also calculated by MSLM-WV and TM using (0.01m, 0.01m, 0.01m) as an approximation of the origin of these events.

Table 7 shows that the calculated locations of MSLM-WV are nearest to the blast site with very similar locations. Absolute distance errors for four events 39, 40, 41 and 43 using MSLM-WV are smaller than the results of using TM, and the maximum deviations are 13.83m and 23.80m, respectively. Absolute distance errors of MSLM-WV for events 39, 41 and 43 are also smaller than the results reported in [37] and [38], and the maximum deviations are 13.83m and 18.60m, respectively.

It can be clearly seen in Table 7 that source location errors are within 12m for three events 39, 41 and 43 using MSLM-WV, while source location errors are within 12m for only one event using TM or the method in [37] and [38]. Therefore, the proposed MSLM-WV gives a better accuracy of source location compared to any of the existing methods.

To clarify the differences between the methods TM and MSLM-WV, Table 8 lists the characteristics, advantages and disadvantages of two methods. It also shows the proposed MSLM-WV is a beneficial complement to the method TM in mines.

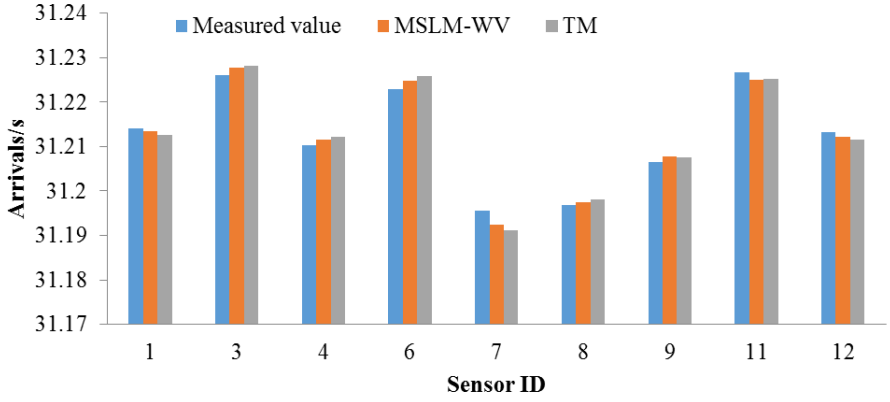


(a)

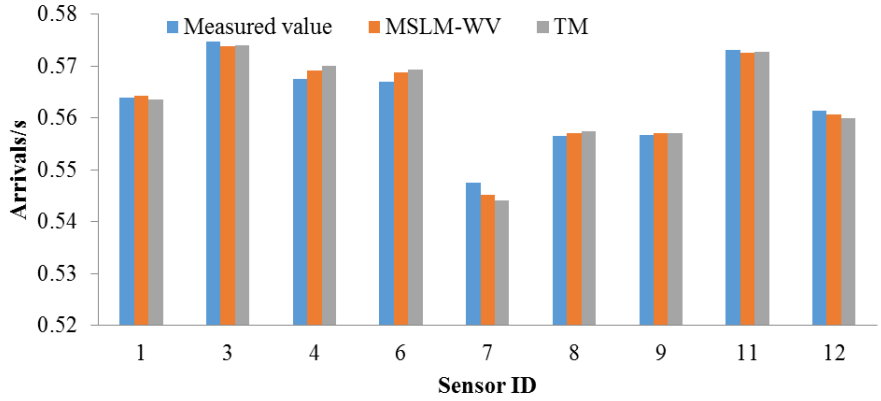


(b)

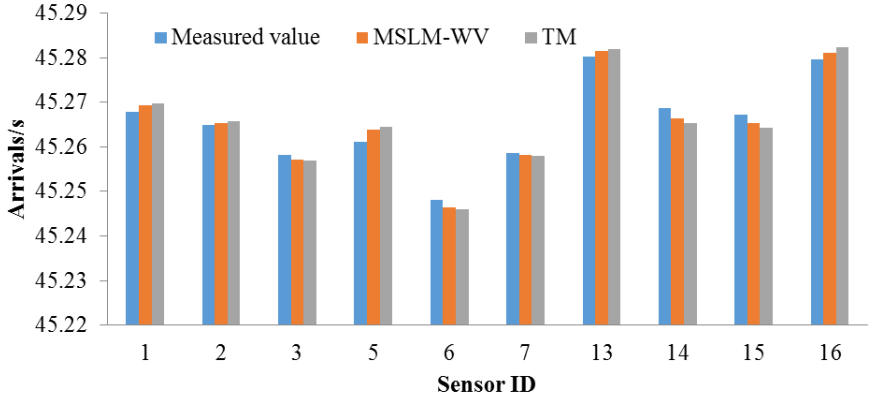


(c)

**FIGURE 6.** (a), (b), and (c) show measured value, fitted values of MSLM-WV and TM for blasting events No.1, No.2, No.3, respectively.

## V. CONCLUSION

A new MS/AE source location method was developed to address the problem of the location error for microseismic monitoring system induced by temporal and spatial errors using the TM with a pre-measured wave velocity. The pencil lead break tests, the thermal fracture experiment in granite, and the blasting experiments (including published examples) were used to verify the proposed method. Both the pencil lead break tests and the thermal fracture experiment have proved that the proposed method without the need for a

pre-measured wave velocity can improve the location accuracy significantly, which is superior to the results of the traditional location method (TM) using pre-measured wave velocity. The results of blasting experiments in Dongguashan copper mine obtained by the MSLM-WV were compared with that by the TM. It shows that the average absolute distance error of the MSLM-WV is 10.16m, whereas the error of the TM is 17.55m. Finally, the MSLM-WV is also applied to published data and it also gives superior results compared to the considered existing methods. It was proved that the proposed MSLM-WV is reasonable and reliable with high location accuracy. Since MSLM-WV method only requires the P wave arrivals, it is more convenient than the method using arrivals of PS waves. Because it can accurately locate the MS/AE source coordinates without the need of a pre-measured velocity, the proposed method can not only decrease the location errors induced by temporal and spatial errors of the wave velocity using the TM, but also determine the location of the MS/AE source in real time, which is a more efficient and effective methodology for detecting faults/breaking signals for both the healthy evaluation and disaster control than the most commonly used TM in mines.

## REFERENCES


[1] M. K. Abdul-Wahed, M. Al Heib, and G. Senfaute, "Mining-induced seismicity: Seismic measurement using multiplet approach and numerical modeling," *Int. J. Coal Geol.*, vol. 66, nos. 1–2, pp. 137–147, Feb. 2006.

[2] L. Driad-Lebeau, F. Lahaie, M. Al Heib, J. Josien, P. Bigarré, and J. F. Noirel, "Seismic and geotechnical investigations following a rockburst in a complex French mining district," *Int. J. Coal Geol.*, vol. 64, nos. 1–2, pp. 66–78, Oct. 2005.

[3] S. Lasocki and B. Orlecka-Sikora, "Seismic hazard assessment under complex source size distribution of mining-induced seismicity," *Tectonophysics*, vol. 456, nos. 1–2, pp. 28–37, Aug. 2008.

[4] A. Leśniak and Z. Isakow, "Space–time clustering of seismic events and hazard assessment in the Zabrze–Bielszowice coal mine, Poland," *Int. J. Rock Mech. Mining Sci.*, vol. 46, no. 5, pp. 918–928, Jul. 2009.

[5] V. A. Mansurov, "Prediction of rockbursts by analysis of induced seismicity data," *Int. J. Rock Mech. Mining Sci.*, vol. 38, no. 6, pp. 893–901, Sep. 2001.

[6] J. Šílený and A. Milev, "Source mechanism of mining induced seismic events—Resolution of double couple and non double couple models," *Tectonophysics*, vol. 456, nos. 1–2, pp. 3–15, Aug. 2008.

[7] L. Z. Tang, C. L. Pan, and X. B. Xie, "Study on rockburst control in deep seated hard ore deposit," *Chin. J. Rock Mech. Eng.*, vol. 22, no. 7, pp. 1067–1071, Jul. 2003.

[8] M. Hudyma and Y. H. Potvin, "An engineering approach to seismic risk management in hardrock mines," *Rock Mech. Rock Eng.*, vol. 43, no. 6, pp. 891–906, Nov. 2010.

[9] Y. Potvin, "Strategies and tactics to control seismic risks in mines," *J. Southern African Inst. Mining Metallurgy*, vol. 109, no. 3, p. 177, Apr. 2009.

[10] J. C. Chen, R. E. Hudson, and K. Yao, "Maximum-likelihood source localization and unknown sensor location estimation for wideband signals in the near-field," *IEEE Trans. Signal Process.*, vol. 50, no. 8, pp. 1843–1854, Aug. 2002.

[11] M. Ge, H. R. Hardy, Jr., H. Wang, and J. Wang, "Development of a simple mechanical impact system as a non-explosive seismic source," *Geotech. Geol. Eng.*, vol. 29, no. 1, pp. 137–142, 2011.

[12] P. Senatorski, "Apparent stress scaling for tectonic and induced seismicity: Model and observations," *Phys. Earth Planetary Interiors*, vol. 167, nos. 1–2, pp. 98–109, Mar. 2008.

[13] N. W. Xu, C. N. Tang, S. H. Wu, G. L. Li, and J. Y. Yang, "Optimal design of microseismic monitoring networking and error analysis of seismic source location for rock slope," *Adv. Mater. Res.*, vols. 163–167, no. 1, pp. 2991–2999, Dec. 2010.

[14] L. Dong, J. Wesseloo, Y. Potvin, and X. Li, "Discrimination of mine seismic events and blasts using the Fisher classifier, naive Bayesian classifier and logistic regression," *Rock Mech. Rock Eng.*, vol. 49, no. 1, pp. 183–211, Jan. 2016.

[15] L. J. Dong, J. Wesseloo, Y. Potvin, and X. B. Li, "Discriminant models of blasts and seismic events in mine seismology," *Int. J. Rock Mech. Min. Sci.*, vol. 86, pp. 282–291, Jul. 2016.

[16] C.-P. Lu, Y. Liu, H.-Y. Wang, and P.-F. Liu, "Microseismic signals of double-layer hard and thick igneous strata separation and fracturing," *Int. J. Coal Geol.*, vols. 160–161, pp. 28–41, Apr. 2016.

[17] L. Dong, X. Li, and G. Xie, "Nonlinear methodologies for identifying seismic event and nuclear explosion using random forest, support vector machine, and naive Bayes classification," *Abstract Appl. Anal.*, vol. 2014, pp. 1–8, Feb. 2014.

[18] B. L. N. Kennett, K. Marson-Pidgeon, and M. S. Sambridge, "Seismic source characterization using a neighbourhood algorithm," *Geophys. Res. Lett.*, vol. 27, no. 20, pp. 3401–3404, Oct. 2000.

[19] Y. Tian and X.-F. Chen, "Review of seismic location study," *Prog. Geophys.*, vol. 17, no. 1, pp. 147–155, Jan. 2002.

[20] P. Nivesrangsan, J. A. Steel, and R. L. Reuben, "Source location of acoustic emission in diesel engines," *Mech. Syst. Signal Process.*, vol. 21, no. 2, pp. 1103–1114, Feb. 2007.

[21] F. Waldhauser and W. L. Ellsworth, "A double-difference earthquake location algorithm: Method and application to the northern Hayward fault, California," *Bull. Seismol. Soc. Amer.*, vol. 90, no. 6, pp. 1353–1368, Dec. 2000.

[22] M. Knapmeyer, "Location of seismic events using inaccurate data from very sparse networks," *Geophys. J. Int.*, vol. 175, no. 3, pp. 975–991, Dec. 2008.

[23] L. Dong, X. Li, L. Tang, and F. Gong, "Mathematical functions and parameters for microseismic source location without pre-measuring speed," *Chin. J. Rock Mech. Eng.*, vol. 30, no. 10, pp. 2057–2067, Oct. 2011.

[24] L.-J. Dong, X.-B. Li, Z.-L. Zhou, G.-H. Chen, and J. Ma, "Three-dimensional analytical solution of acoustic emission source location for cuboid monitoring network without pre-measured wave velocity," *Trans. Nonferrous Met. Soc. China*, vol. 25, no. 1, pp. 293–302, Jan. 2015.

[25] L. Dong, X. Li, and G. Xie, "An analytical solution for acoustic emission source location for known P wave velocity system," *Math. Problems Eng.*, vol. 2014, pp. 1–6, Mar. 2014.

[26] T. Kundu, "Acoustic source localization," *Ultrasonics*, vol. 54, no. 1, pp. 25–38, Jan. 2014.

[27] T. Kundu, H. Nakatani, and N. Takeda, "Acoustic source localization in anisotropic plates," *Ultrasonics*, vol. 52, no. 6, pp. 740–746, Aug. 2012.

[28] X. Li and L. Dong, "An efficient closed-form solution for acoustic emission source location in three-dimensional structures," *Aip Adv.*, vol. 4, no. 2, p. 027110, Feb. 2014.

[29] L. Dong, W. Shu, X. Li, G. Han, and W. Zou, "Three dimensional comprehensive analytical solutions for locating sources of sensor networks in unknown velocity mining system," *IEEE Access*, vol. 5, pp. 11337–11351, May 2017.

[30] G. L. Pavlis and J. R. Booker, "The mixed discrete-continuous inverse problem: Application to the simultaneous determination of earthquake hypocenters and velocity structure," *J. Geophys. Res.*, vol. 85, no. B9, pp. 4801–4810, Sep. 1980.

[31] X. Li and L. Dong, "Comparison of two methods in acoustic emission source location using four sensors without measuring sonic speed," *Sensor Lett.*, vol. 9, no. 5, pp. 2025–2029, Oct. 2011.

[32] Q.-Y. Li, L.-J. Dong, X.-B. Li, Z.-Q. Yin, and X.-L. Liu, "Effects of sonic speed on location accuracy of acoustic emission source in rocks," *Trans. Nonferrous Met. Soc. China*, vol. 21, no. 12, pp. 2719–2726, Dec. 2011.

[33] J. A. Nelder and R. Mead, "A simplex method for function minimization," *Comput. J.*, vol. 8, no. 1, pp. 308–313, Jan. 1965.

[34] I. Jordanov and A. Georgieva, "Neural network learning with global heuristic search," *IEEE Trans. Neural Netw.*, vol. 18, no. 3, pp. 937–942, May 2007.

[35] K. Levenberg, "A method for the solution of certain problems in least squares," *Quart. Appl. Math.*, vol. 2, no. 2, pp. 164–168, 1944.

[36] D. W. Marquardt, "An algorithm for least-squares estimation of nonlinear parameters," *J. Soc. Ind. Appl. Math.*, vol. 11, no. 2, pp. 431–441, 1963.

[37] M. Ge, "Efficient mine microseismic monitoring," *Int. J. Coal Geol.*, vol. 64, nos. 1–2, pp. 44–56, Oct. 2005.

[38] M. Ge, "Source location error analysis and optimization methods," *J. Rock Mech. Geotech. Eng.*, vol. 4, no. 1, pp. 1–10, Apr. 2012.

**LONGJUN DONG** (M'16) received the Ph.D. degree from the School of Resources and Safety Engineering, Central South University, Changsha, China, in 2013. From 2012 to 2013, he was an Assistant Researcher with the Australia Center for Geomechanics, The University of Western Australia, Perth, WA, Australia. His current research interests include computational methods in location and identification for shock sources, seismic signals, machine learning algorithms, and rock/mineral mechanics for mining science.

He is currently an Associate Professor with the School of Resource and Safety Engineering, Central South University, China. He is a member of ASCE and ISRM. He was selected for The Young Elite Scientifics Sponsorship Program by the China Association for Science and Technology. He is invited to serve as the Editorial Board Member of *Scientific Reports*, *Internal Journal of Distributed Sensor Networks*, and *Shock and Vibration*.

**DAOYUAN SUN** received the B.Sc. degree in mining engineering from Central South University, Changsha, China, in 2015, where he is currently pursuing the M.Sc. degree. His research interests include rock mechanics, microseismic monitoring, and microseismic/AE source locating method.

**XIBING LI** received the Ph.D. degree in mining engineering from the Central South University of Technology, Changsha, China, in 1992. He was a Senior Visiting Scholar with the Rock Mechanics and Explosives Research Center, University of Missouri Rolla from 1998 to 1999. He was also a Researcher with NanYang Technological University, Singapore, from 1999 to 2001. He received four projects of National Science and Technology Award, and 14 projects of Provincial/Ministerial Science and Technology Award. He was selected for ''The National Science Fund for Distinguished Young Scholars'' and ''Chang Jiang Distinguished Professor.'' He received the National Award for Youth in Science and Technology and the National Excellent Scientific and Technological Worker.

Dr. Li has been the Committee Member with the Rock Dynamics of the International Society for Rock Mechanics since 2008. He has also been the Vice President of the Chinese Society for Rock Mechanics and Engineering since 2016.

**KUN DU** received the Ph.D. degree from Central South University, Changsha, China, in 2013. Since 2014, he has been a Post-Doctoral Researcher with the Postdoctoral Scientific Research Workstation, Shenzhen Zhongjin Lingnan Nonfemet Co., Ltd. His current research interest is rock mechanics and deep mining technology.

He is currently an Associate Professor with the School of Resources and Safety Engineering and Advanced Research Center, Central South University. He is the author of over 20 papers published in related international conference proceedings and journals, and is the holder of three patents. He received two first class prizes of Scientific and Technological Progress Award from the China Gold Association in 2016. He has served as a reviewer of more than ten journals.